Proceedings of the 35th
Conference on Decision and Control
Kobe, Japan • December 1996

An Experimental Study on Modelling and Identification of Harmonic Drive Systems

H.D. Taghirad† and P.R. Bélanger‡
Center for Intelligent Machines,
Department of Electrical Engineering,
McGill University, Montréal, H3A 2A7
† taghirad@cim.mcgill.ca, ‡ pbelange@fgsr.lan.mcgill.ca

Abstract

Despite widespread industrial application of harmonic drives, mathematical representation of their dynamics has not been fully addressed. In this theoretical/experimental study of harmonic drive systems a systematic way to capture and rationalize the dynamics of the system is proposed. Simple and accurate models for compliance, hysteresis, and friction are given and the model parameters are estimated from experiments using least square approximation. A statistical measure of consistency is defined, by which the reliability of the estimated parameter for different operating condition, as well as the accuracy and integrity of the proposed model is quantified. The validity of the modelling scheme is finally evaluated, on two different harmonic drives by comparing the experimental and simulation results.

1 Introduction

Since its inception in 1955, the harmonic drive has found widespread acceptance among practitioners. This mechanical transmission, occasionally called "strain-wave gearing", employs a continuous deflection wave along *non-rigid gear* to allow for gradual engagement of gear teeth (Figure 1). Because of this unconventional gear-tooth meshing action, harmonic drives can deliver high reduction ratios in a very small package. In fact, the radical mechanical operation of this gear train defies conventional understanding of gear behaviour and creates a new arena for exploration and understanding.

The harmonic drive exhibits performance features both superior and inferior to conventional gear transmissions. Its performance advantages include high torque capacity, concentric geometry, lightweight and compact design, zero backlash, high efficiency, and back drivability. Harmonic drive systems suffer however, from high flexibility, resonance vibration, friction and structural damping nonlinearities. The lack of literature, relative to that for conventional gear transmission also inhibit their use. The unique performance features of the harmonic drive have captured the attention of designers in many fields. It has been used in industrial and space robots, assembly equipment, and measuring instruments, as well as heavy duty applications such as machine tools and printing presses. Additionally, space and aircraft systems often employ harmonic drives for their light weight and compact geometry.

Throughout its short existence, the harmonic drive has enjoyed increasing international attention from designers as well as researchers. The Russians were perhaps the first who initiated substantial research on the dynamic behavior of harmonic drives [1, 2]. More recently Tuttle and Seering performed an extensive effort to model the stiffness, positioning accuracy, gear tooth-meshing mechanism and friction of the harmonic drive [3, 4]. Their experimental observations show that the velocity response to step commands in motor current are not only contaminated by serious vibration, but also by unpredictable jumps. The velocity response observations were used to guide the development of a series of models with increasing complexity to describe the harmonic drive behavior. Their most complex model involved kinematic error, nonlinear stiffness, and gear-tooth interface with frictional losses.

Kircanski and Goldenberg have also attempted to model the harmonic drive in detail [5]. They used the drive system in contact with a stiff environment, in contrast to unrestrained motion experiments used in [4], and illustrated that in this case nonlinear stiffness, hysteresis and friction are more tractable. Simple models for soft-windup, hysteresis, and friction were proposed and the parameters were identified by restrained motion experiments.

Hsia [6], Legnani [7], Marilier [8], and Seyfferth [9] are among others who attempted to model the stiffness, friction, and position accuracy of harmonic drive sys-

0-7803-3590-2/96 $5.00 © 1996 IEEE

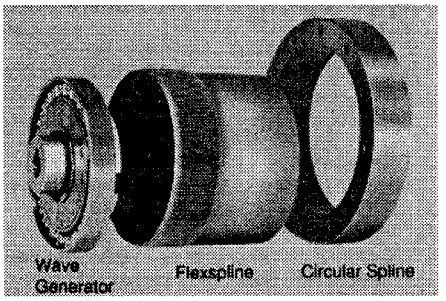

Figure 1: Harmonic drive components

tems. All these researchers noted the inherent difficulties in finding an accurate model for the system.

In this paper a moderately complex model of harmonic drive system is developed. Restrained and unrestrained motion experiments are use to identify the model parameters and illustrate the fidelity of the model for two different types of harmonic drive systems. It is shown that a linear stiffness model for stiffness combined with a velocity dependent structural damping model can replicate the hysteresis torsion curve of the system for restrained motion experiments. The frictional losses of the transmission has been modelled using Coulomb friction, Viscous damping and Stribeck friction. Both high speed, and low speed friction terms has been identified using unrestrained and restrained motion experiments respectively. Finally, the simulation of the system built in Simulink has been used to verify the model by experiments. It has been verified that the simulation accurately predicts the restrained and unrestrained experiments.

2 Experimental Setup

Two harmonic drive testing stations were used to monitor the behaviour of two different harmonic drives. A picture of the setup and its schematics are illustrated in Figure 2, in which the harmonic drive is driven by a DC motor, and a load inertia is used to simulate the robot arm for unrestrained motion. Also a positive locking system is designed such that the output load can be locked to the ground. In the first experimental setup, the circular spline is fixed to the ground and the output is carried by the flexspline, while in the other setup, the flexspline is fixed and the circular spline is used for output rotation. By this arrangement the behavior of the transmission under different operating configurations can be observed. Each setup is equipped with a tachometer to measure the motor velocity, and an encoder on the load side to measure the output position. The output torque is measured by a Wheatstone bridge of strain gauges mounted directly on the flexspline [10], and the current applied to the DC motor is measured

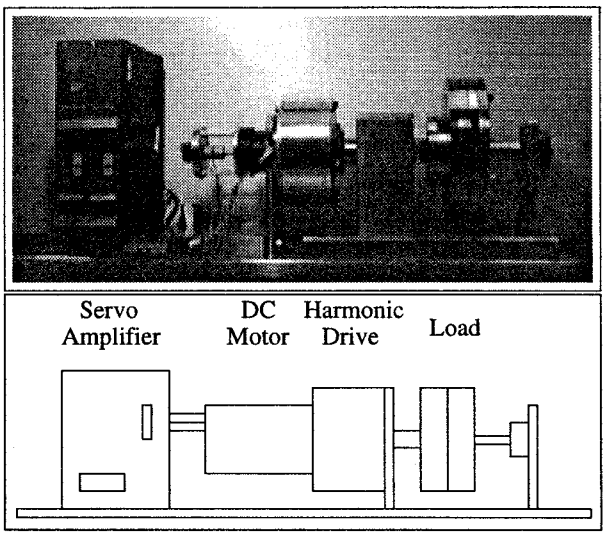

Figure 2: A picture of the experimental setup and its schematics

from the servo amplifier output. To obtain an estimate of the output velocity, a Kalman filter estimator on encoder readings [11], is employed. These signals were processed by several data acquisition boards and monitored by a C-30 Challenger processor executing compiled computer C codes.

3 Modelling and Identification

The goal of modelling the harmonic drive system is to discover the simplest representation which can replicate system performance to a desired level of accuracy. A computer model will be the basis for discovering and examining proposed control algorithms, before implementing them in practice. Usually a simple model could serve as the basis for the controller design. However, in this paper a rather complete model of the system is created to aid understanding of the system. In practice it has been proven that the knowledge obtained through the process of modelling and identification of the system becomes a powerful medium for understanding, and improving the design, as well as for providing new horizons for controller design.

3.1 DC–Motor

A DC motor can be viewed as a two input, one output black box, where the servo current and external torque are the inputs and the angular displacement (or velocity) is the output. The torque balance for the DC motor can be written in the form:

$$K_m i = J_m \ddot{\theta} + T_{f_m} + T_{out} \quad (1)$$

where K_m is the motor torque constant, i is the in-

	DC Motor 1		DC Motor 2	
	Estimated Parameter	Consist. Measure	Estimated Parameter	Consist. Measure
K_m	0.0542	0%	0.1815	0%
J_m	5.5×10^{-5}	0.82%	5.8×10^{-5}	5.75%
T_{v_p}	5.3×10^{-5}	23.3%	8.6×10^{-4}	7.75%
T_{v_n}	5.3×10^{-5}	11.5%	5.8×10^{-4}	14.4%
T_{s_p}	1.4×10^{-2}	9.01%	1.5×10^{-2}	25.9%
T_{v_p}	1.3×10^{-2}	5.72%	2.7×10^{-2}	25.8%

Table 1: DC motors estimated parameters

put current to the motor, J_m is the motor inertia, and T_{out} is the external torque. T_{f_m} is the friction torque, which can be modelled in the form of velocity direction dependent viscous and Coulomb friction as follows:

$$T_{f_m}(\dot{\theta}) = T_{v_n} u_{-1}(-\dot{\theta})\dot{\theta} + T_{v_p} u_{-1}(\dot{\theta})\dot{\theta} + T_{s_n} u_{-1}(-\dot{\theta})\text{sign}(\dot{\theta}) + T_{s_p} u_{-1}(\dot{\theta})\text{sign}(\dot{\theta}) \quad (2)$$

where

$$u_{-1}(x) = \begin{cases} 1 & \text{if } x > 0 \\ 0 & \text{if } x \leq 0 \end{cases} \quad (3)$$

Note that the indices p and n represents the dependence of the friction coefficients on the velocity direction.

The model parameters are estimated by least square approximation. Using Equation 1 as a linear regression model, and measuring the motor velocity and current for two sets of high and low velocity experiments, the model parameters can be estimated using *Moore–Penrose generalized inverse* [12, 13]. Householder reflection is utilized in numerical calculations to avoid ill conditioning [14].

By means of least square estimation, for each experiment we obtained a set of parameters. However, these

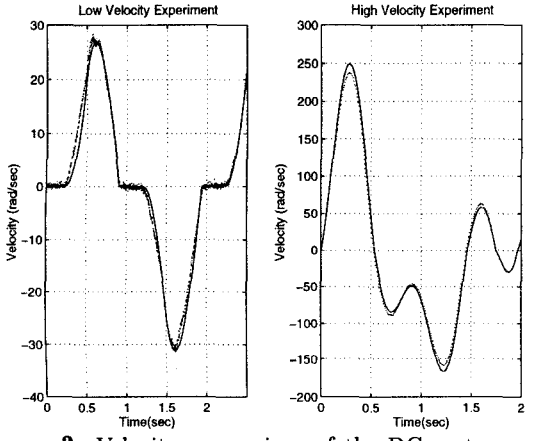

Figure 3: Velocity comparison of the DC motor model and experiment for two typical experiments

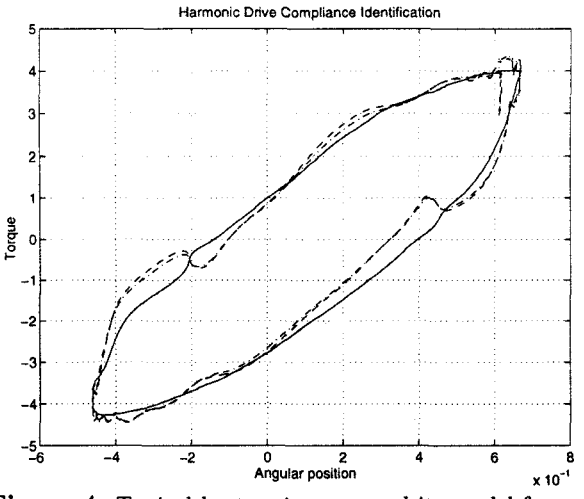

Figure 4: Typical hysteresis curve and its model for optimal α (dash-dot), and $\alpha = \frac{1}{2}$ (dashed)

parameters are deemed acceptable, only if they are consistent for other experiments. By consistency we mean a statistical measure, namely *the ratio of the standard deviation to the average value of each parameter estimated for different experiments.* If this measure is small, we have a good consistency for different experiments, and in other words, the model is good enough to capture the dynamics of the system.

Figure 3 illustrates the velocity fit obtained by the model for two typical experiments. The model is capable of capturing the dynamics of the system for both low and high velocity experiments. Table 1 summarizes the estimation results for two setup DC motors. Note that the motor torque constant K_m is obtained from the motor specs, and assumed to be known in the least square estimation. The consistency measure of the results for different experiment shows less than 10% for some parameters, and less than 30% for others. The reason for variation in consistency measure among parameters is that some experiments are not persistently exciting to estimate those friction coefficients. However, it has been verified by simulations that having consistency measure less than 30% gives relatively good match to the experiments.

3.2 Harmonic Drive Compliance

As described in a manufacturer's catalogue [15], a typical shape of the harmonic drive compliance curve is given in Figure 4. This curve illustrates harmonic drive nonlinear stiffness and hysteresis. To capture the nonlinear stiffness behavior, manufacturers suggest using piecewise linear approximations [15], whereas other researchers prefer a cubic polynomial approximation [4, 2]. The hysteresis effect, however, is more difficult

to model, and consequently it is often ignored. Recently Seyfferth et al. proposed a fairly complex model to capture the hysteresis [9]. The hysteresis in the harmonic drive compliance profile may be explained by structural damping of the flexspline. The inherent coupling of stiffness torque and structural damping, therefore, make it very hard to identify those separately. We suggest that Figure 4 is in fact a Lissajous figure, and we identify both the stiffness and damping of the flexspline together using least square estimation. Linear and cubic models for compliance and many different models for structural damping were tried in this framework. Dahl model for friction [16, 17], Duham, Preisach and Babuska models for hysteresis [18], are among the dynamic models used to replicate the hysteresis torsion curve. We observed, however, that a linear stiffness model with a static model, relating the structural damping to a power of the velocity can best capture hysteresis behavior. Equation 4 gives in detail the compliance model, where $\Delta\theta$ is the flexspline relative torsion.

$$T_{meas} = K_1\Delta\theta + T_{st}|\Delta\dot{\theta}|^{\alpha}\text{sign}(\Delta\dot{\theta}) \qquad (4)$$

To identify the model parameters, a set of restrained motion experiments has been employed, in which the torque T_{meas} and the motor velocity has been measured. Equation 4 forms a nonlinear regression in which K_1, T_{st} and α are unknown. Using an iterative least square solution for this nonlinear regression model, it is found that the optimal estimate of α is very close to 0.5. Consequently the damping torque of the system can be related to the square root of the relative torsion velocity. Figure 4 illustrates a typical hysteresis torsion curve fitted by the model, comparing the difference between the optimal α and $\alpha = \frac{1}{2}$. By fixing the value of $\alpha = \frac{1}{2}$, Equation 4 forms a linear regression model for the system, that can be solved for different experiments. Table 2 summarizes the compliance parameter for the harmonic drives of our two setups.

3.3 Harmonic Drive Friction

All harmonic drives exhibit power loss during operation due to transmission friction. Figure 5 illustrates the schematics of the harmonic drive model. The bulk

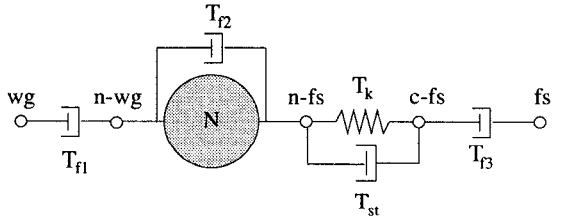

Figure 5: Transmission model of harmonic drive with compliance and friction

	Harmonic Drive 1		Harmonic Drive 2	
	Estimated Parameter	Consist. Measure	Estimated Parameter	Consist. Measure
α	$\frac{1}{2}$	0%	$\frac{1}{2}$	0%
K_1	6340	9.6%	104.2	4.36%
T_{st}	57.2	28.2%	7.96	28.0%
J_{eff}	1.0×10^{-4}	6.38%	1.0×10^{-4}	8.72%
T_{v_p}	3.7×10^{-4}	16.7%	1.8×10^{-3}	13.2%
T_{v_n}	3.5×10^{-4}	19.3%	2.1×10^{-3}	8.42%
T_{s_p}	4.6×10^{-2}	23.7%	7.5×10^{-2}	29.2%
T_{s_n}	4.4×10^{-2}	24.0%	3.3×10^{-2}	30.8%
$T_{ss_{p1}}$	−0.0076	14.7%	−0.0487	20.3%
$T_{ss_{n1}}$	−0.0203	23.8%	−0.0450	18.6%
T_{ss_2}	0.1	0%	0.1	0%

Table 2: Harmonic drive estimated parameters

of energy dissipation can be blamed on the wave generator bearing friction T_{f_1}, gear meshing friction T_{f_2}, output bearing frictions T_{f_3} and the flexspline structural damping T_{st}. Among them, most of the frictional dissipation results from gear meshing. Also comparing the ball bearing frictions, T_{f1} is more important than T_{f_3} since it is acting on the high speed/low torque port of transmission, and its effect on the dynamics of the system is magnified by the gear ratio. The transmission torque is measured on the flexspline (namely node c_{fs} of Figure 5). The torque balance, therefore, can be written as:

$$T_{wg} = \frac{1}{N}(T_{meas}) + T_{f_1} + T_{f_2} \qquad (5)$$

in which the measured torque $T_{meas} = T_k + T_{st}$, N is the gear ratio, and T_{wg} is the resulting torque of wave generator, provided by the DC motor. From Equation 1, T_{wg} can be related to the input current by:

$$T_{wg} = K_m i - J_m\ddot{\theta} - T_{f_m} \qquad (6)$$

Thus, the final torque balance of the system is the following:

$$K_m i - \frac{1}{N}T_{meas} = J_{eff}\ddot{\theta}_{wg} + (T_{f_m} + T_{f_1} + T_{f_2}) \qquad (7)$$

in which K_M is the motor torque constant, J_{eff} is the effective input inertia, and T_{f_m} is the motor friction. The gear meshing friction torque is modelled as Coulomb, viscous and Stribeck friction [19, 20], having velocity direction dependent coefficient as follows:

$$\begin{aligned} T_{f_2} &= T_{v_p}\dot{\theta}_{wg}\, u_{-1}(\dot{\theta}_{wg}) + T_{v_n}\dot{\theta}_{wg}\, u_{-1}(-\dot{\theta}_{wg}) + \\ &T_{s_p}\text{sign}(\dot{\theta}_{wg})\, u_{-1}(\dot{\theta}_{wg}) + T_{s_n}\text{sign}(\dot{\theta}_{wg})\, u_{-1}(-\dot{\theta}_{wg}) + \\ &T_{ss_{p1}}\text{sign}(\dot{\theta}_{wg})\, u_{-1}(\dot{\theta}_{wg}) e^{-\left(\frac{\dot{\theta}_{wg}}{T_{ss_{p2}}}\right)^2} + \\ &T_{ss_{n1}}\text{sign}(\dot{\theta}_{wg})\, u_{-1}(-\dot{\theta}_{wg}) e^{-\left(\frac{\dot{\theta}_{wg}}{T_{ss_{n2}}}\right)^2} \end{aligned} \qquad (8)$$

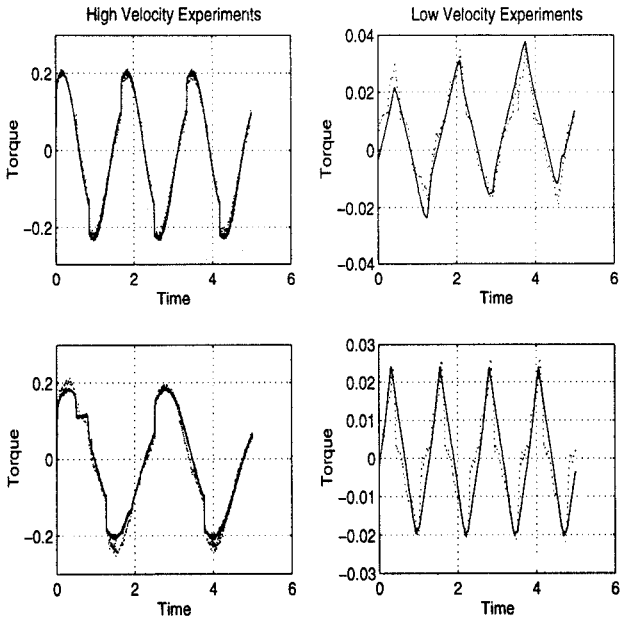

Figure 6: Comparison of harmonic drive modelled and experimented torque; dotted: experiment, solid: modelled

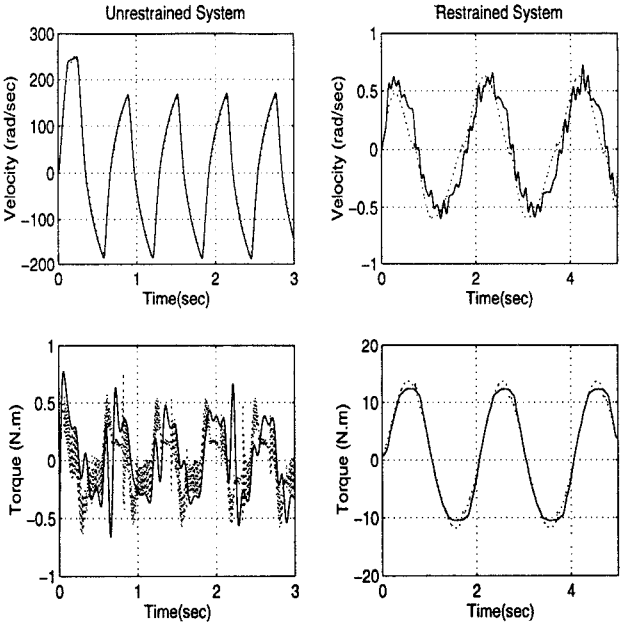

Figure 7: Simulation verification for restrained and unrestrained systems; Solid : Simulation, Dotted : Experiment

The Stribeck model for friction can capture the dynamics of the friction at low velocities. Unlike compliance identification, both restrained and unrestrained experiments are employed to identify the friction model parameters. Unrestrained experiments are persistently exciting for viscous and Coulomb friction, while restrained motion experiments operate the system at low velocities which is ideal for Stribeck coefficient identification. Unrestrained low velocity experiments are used as well, for Stribeck coefficient identification. Equation 7 forms a linear regression model for the high velocity experiments in the absence of the nonlinear Stribeck terms. It should be noted that in this regression model instead of the internal system friction T_{f_m}, T_{f_1} and T_{f_2}, the entire friction of the system ($T_f = T_{f_m} + T_{f_1} + T_{f_2}$), can be identified. This imposes no limitation on the identification procedure, since only the entire friction T_f is required for the simulations. For low velocity experiment also, Equation 7 can provide a linear regression if T_{ss_2} is assumed to be known. Figure 6 illustrates the torque fit obtained for four typical experiments. Table 2 summarizes the estimate friction parameters of two harmonic drives assuming fixed $T_{ss_2} = 0.1$, and their consistency measure. The consistency measure for all parameters are less than 30%, which indicates the reliability of the estimated parameters. It is important to note that the estimated Stribeck friction coefficients are negative, which is in contrary to the usual dynamics of friction reported at at low velocity [21, 22]. However, this illustrates that there is no stiction in the harmonic drive transmission, verifying the manufacturers claim [23], nevertheless, it represents rising friction at low velocities.

4 Modelling Scheme Verification

To verify the model validity, simulations of the system for both restrained and unrestrained systems is developed in Simulink. The simulation input is the measured current experimented on the system, as well as the identified parameters reported in Section 3. The output velocity and torque of the system is compared to typical experimented outputs in Figure 7. For unrestrained system, there is a perfect match for the velocity, and relatively good match for torque curves. For restrained system, the match between velocities is less accurate, and this is because of the smaller velocity signal and larger noise to signal ratio. However, the resulting torques are quite similar. This was verified for more than twenty other experiments for both harmonic drives, and all of them show a similar match between experiment and simulation. The accurate match between simulation and experiment for different operating ranges, indicates the fidelity of the model to accurately replicate the dynamic behavior of the system.

5 Conclusions

Based on experimental and theoretical studies, a systematic way to capture and rationalize the dynamics of the harmonic drive systems is introduced. Simple and accurate models for compliance, hysteresis, and friction are established and model parameters are iden-

tified using least square approximation. A measure of consistency is defined, by which the reliability of the estimated parameter for different operating condition, as well as the accuracy of the simple model is quantified. From compliance modelling results, it has been illustrated that identifying stiffness and structural damping together will resolve the reported difficulties in determining the compliance parameters. Moreover, it has been shown that a linear stiffness model best captures the behavior of system when combined with a good model for hysteresis. A simple static model for hysteresis is also introduced, and it is shown that this simple model can replicate the hysteresis effect in harmonic drives better than some other dynamic models reported in the literature. Friction losses of the harmonic drive are modelled at both low velocity and high velocity operating regimes. From experiments on two different harmonic drives it has been observed that there is no stiction in the transmission, but rather a rising friction acts at low velocities. Finally, the model performance is assessed by a simulation verifying the experimental results for both restrained and unrestrained systems.

References

[1] N.A. Aliev. A study of the dynamic behavior of flexible gears in harmonic drives. *Soviet Engineering Research*, 66(6):7–11, 1986.

[2] D.P. Volkov and Y.N. Zubkov. Vibration in a drive with harmonic gear transmission. *Russian Engineering Journal*, 58(5):17–21, 1978.

[3] T.D. Tuttle. Understanding and modeling the behavior of a harmonic drive gear transmission. Technical Report 1365, MIT Artificial Intelligence Laboratory, 1992.

[4] T.D. Tuttle and W. Seering. Modeling a harmonic drive gear transmission. *Proceeding of IEEE International Conference on Robotics and Automation*, 2:624–629, 1993.

[5] N. Kircanski, A. Goldenberg, and S. Jia. An experimental study of nonlinear stiffness, hysteresis, and friction effects in robot joint with harmonic drives and torque sensors. *Proceedings of the Third International Symposium on Experimental Robotics*, 1:147–154, 1993.

[6] L. Hsia. The analysis and design of harmonic gear drives. *Proceedings of the 1988 IEEE International Conference on Systems, Man and Cybernetics*, 1:616–619, 1988.

[7] G. legnani and R. Faglia. Harmonic drive transmission: the effect of their elasticity, clearance and irregularity on the dynamic behaviour of an actual SCARA robot. *Robotica*, 10:369–375, October 1992.

[8] T. Marilier and J.A. Richard. Non-linear mechanic and electric behavior of a robot axis with a harmonic-drive gear. *Robotics and Computer-Integrated Manufacturing*, 5(2/3):129–136, 1989.

[9] W. Seyfferth, A.J. Maghzal, and J. Angeles. Nonlinear modeling and parameter identification of harmonic drive robotic transmissions. *Proceeding of IEEE International Conference on Robotics and Automation*, 3:3027–3032, 1995.

[10] M. Hashimoto, Y. Kiyosawa, H. Hirabayashi, and R.P. Paul. A joint torque sensing technique for robots with harmonic drives. *Proceeding of IEEE International Conference on Robotics and Automation*, pages 1034–1039, April 1991.

[11] P.R. Belanger. Estimation of angular velocity and acceleration from shaft encoder measurements. Technical Report TR-CIM-91-1, Center for Intelligent Machines, 1991.

[12] K.L. Doty, C. Melchiorri, and C. Bonivento. Theory of generalized inverses applied to robotics. *International Journal of Robotics Research*, 12(1):1–19, Feb 1993.

[13] A. Ben-Israel. *Generalized Inverses: Theory and Application.* Wiley, New York, 1974.

[14] G.H. Golub and C. Van Loan. *Matrix computations.* The Johns Hopkins University Press, Baltimore, MD, 1983.

[15] HD Systems Inc. Harmonic drive gearing. *HD Systems Catalogue*, 1991.

[16] P.R. Dahl. Solid friction damping of mechanical vibration. *AIAA Journal*, 14(12):1675–1682, December 1976.

[17] D.C. Threlfall. The inclusion of coulomb friction in mechanisms programs with particular reference to DRAM. *Mech. and Mach. Theory*, 13:475–483, 1978.

[18] J.W. Macki, P. Nistri, and P. Zecca. Mathematical models for hysteresis. *SIAM Review*, 35(1):94–123, March 1993.

[19] B. Armstrong-Helouvry, P. Dupont, and C. Canudas de wit. A survey of models, analysis tools and compensation methods for control of machines with friction. *Automatica*, 30(7):1083–1138, 1994.

[20] A. Tustin. The effects of backlash and speed-dependent friction on the stability of closed-cycle control systems. *J. Inst. Elec. Eng.*, 94(2A):143–151, 1947.

[21] B. Armstrong-Helouvry. Stick slip and control in low speed motion. *IEEE Transactions on Automatic Control*, 38(10):1483–1496, October 1993.

[22] D.P. Hess and A. Soom. Friction at a lubricated line contact operating at oscillating sliding velocities. *Journal of Tribology*, 112(1):147–152, January 1990.

[23] J.H. Charlson. Harmonic drives for servomechanisms. *Machine design*, 57(1):102–106, January 1985.